

# International Conference on Space Optics—ICSO 2008

Toulouse, France

14–17 October 2008

*Edited by Josiane Costeraste, Errico Armandillo, and Nikos Karafolas*



## ***Status of AlGaN based focal plane array for near UV imaging and strategy to extend this technology to far-UV by substrate removal***

*Jean-Luc Reverchon*

*Yves Gourdel*

*Jean-Alexandre Robo*

*Jean-Patrick Truffer*

*et al.*



# STATUS OF AlGaN BASED FOCAL PLANE ARRAY FOR NEAR UV IMAGING AND STRATEGY TO EXTEND THIS TECHNOLOGY TO FAR-UV BY SUBSTRATE REMOVAL

Jean-Luc Reverchon<sup>(1)</sup>, Yves Gourdel<sup>(1)</sup>, Jean-Alexandre Robo<sup>(2)</sup>, Jean-Patrick Truffer<sup>(2)</sup>, Eric Costard<sup>(2)</sup>, Julien Brault<sup>(3)</sup>, Jean-Yves Duboz<sup>(3)</sup>

(1) Thales Research and Technology, RD 128, 91767 Palaiseau, France, [jean-luc.reverchon@thalesgroup.com](mailto:jean-luc.reverchon@thalesgroup.com)

(2) GIE Alcatel- Thales 3-5lab, RD 128, 91767 Palaiseau Cedex, France

(3) CNRS-CRHEA, rue Bernard Grégory, 06560 Valbonne, France

## ABSTRACT

The fast development of nitrides has given the opportunity to investigate AlGaN as a material for ultraviolet detection. Such AlGaN based camera presents an intrinsic spectral selectivity and an extremely low dark current at room temperature.

Firstly, we will present results on focal plane array of 320x256 pixels with a pitch of 30 $\mu$ m. The peak responsivity is around 280nm (solar-blind), 310nm and 360nm. These results are obtained in a standard SWIR supply chain (readout circuit, electronics).

With the existing near-UV camera grown on sapphire, the short wavelength cutoff is due to a window layer improving the material quality of the active layer. The ultimate shortest wavelength would be 200nm due to sapphire substrate. We present here the ways to transfer the standard design of Schottky photodiodes from sapphire to silicon substrate. We will show the capability to remove the silicon substrate, and etch the window layer in order to extend the band width to lower wavelengths.

## 1. AlGaN SUPPLY CHAIN

### 1.1. Material and optoelectronic aspects

AlGaN on silicon carbide or silicon substrate already exists for microwave applications whereas AlGaN on sapphire is dedicated to LEDs and lasers. Many papers have concerned our UV imagers development<sup>1,2,3,4</sup>. It concerns choice of photodiodes, architecture and material growth difficulties when achieving devices with high aluminum contents.

Schottky and p-i-n photodiodes present large quantum efficiency without biasing. Schottky photodiodes are less popular than p-i-n photodiodes. A disadvantage is the internal photoemission that limits the solar blindness and a smaller build in electric field than in p-n junctions. The advantage is the absence of p-doped material. Indeed, p doping is very difficult in AlGaN with a high Al content. Solar blind p-i-n junction actually uses p GaN that limits the rejection ratio at 360 nm.

Consequently, rejection in visible is considerably altered. On the contrary, Schottky photodiodes only requires n doping of the window layer.

Results from Current-Voltage characterization show that leakage exists on mesa edges. Nevertheless,  $R_0A$  are larger than  $5 \cdot 10^9$  ( $\Omega \cdot \text{cm}^2$ ). No dark current is observed with focal plane arrays. Rejection of sub-band gap responsivity, limitation is always internal photoemission in the contacts<sup>6</sup>.

Another advantage of Schottky photodiodes in the case of 2D arrays is that it doesn't require mesa etching. Schottky contact collect carriers without damaging the Modulation Transfer Function.

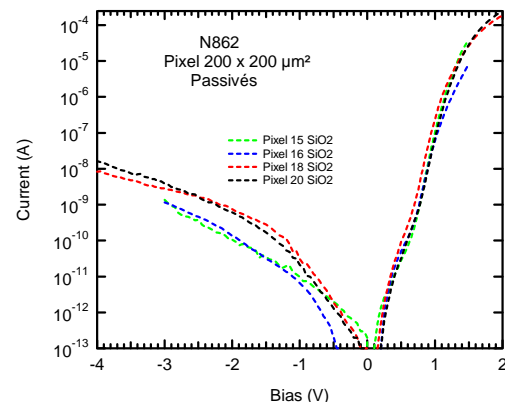


Fig. 1: Current-voltage curves

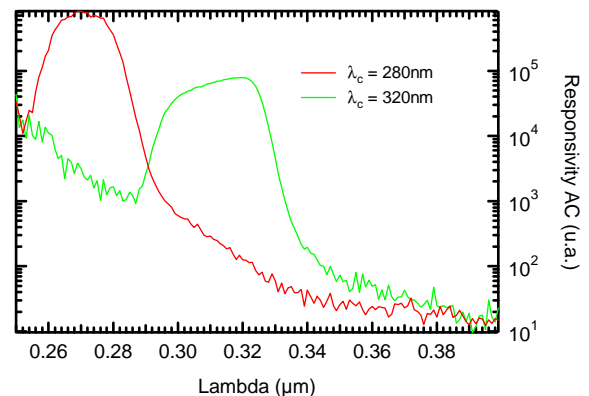


Fig. 2: Spectral response on mono-elements used for Focal Plan Array (FPA)

## 1.2. Focal Plane based on AlGaIn array

Next realizations described here after consist in UV focal plane array fully compatible with standard supply chain, for example InGaAs imaging technology. Readout circuit and electronics are common to InGaAs supply chain.

Non-uniformity of peak response wavelength and quantum efficiency are lower than 5% without any correction. The zero bias operation with 30% quantum efficiency makes these devices compatible with standard infrared readout circuits and SWIR supply chain.

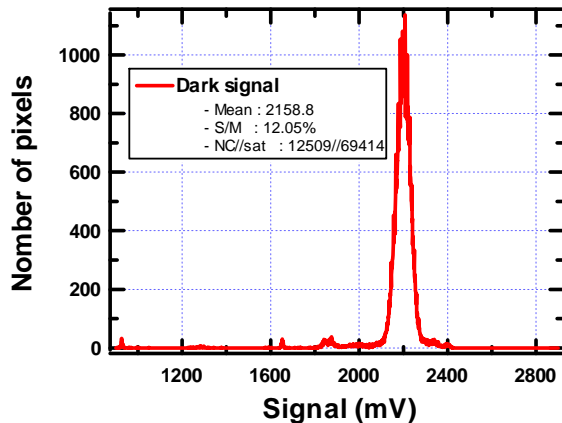


Fig. 3: Histogram of dark signal

We will demonstrate imagers based on the readout circuit ISC 9809 in chapter 2. This multiplexor is dedicated to low level application with two gain modes. It is based on 320 x256 pixels with a pitch of 30 $\mu$ m. The maximum full frame rate is 346Hz @5MHz. NTSC and PAL video output, windowing and skimming capabilities are allowed. The electrical capabilities of AlGaIn technologies to detect extremely low UV signal are currently limited by the ROIC capabilities. The measured electrical noise is 750 e-rms with 1mV/e- gain whereas value as low as 50 e-rms is achieved with gain of 20mV/e-.

Multiplexing is achieved via a readout integrated circuit (ROIC) ISC9809 from Indigo Systems. It consists in a 2D array of 320 x256 pixels with a 30 $\mu$ m pitch. The ISC9809 is especially adapted for very low background conditions.

A capacitive trans-impedance amplifier input circuit (CTIA) provides a low noise front end including an anti-blooming transistor. The input CTIA has two selectable integration capacitors (10 and 210 fF) handling a charge capacity range of 0.17 $\times 10^6$  and 3.5 $\times 10^6$  electrons respectively.

In the hybridization process indium is initially deposited on the ROIC wafers. One critical point in the hybridization turned out to be the presence of strain in the AlGaIn layer leading to a bowing of the AlGaIn chip, which has an area of about 1cm<sup>2</sup>.

Hence, it was essential to optimize the temperature and pressure variations during the hybridization process. After some iteration, a hybridization yield close to 100% was reached. We have measured the temporal and spatial noise in the array.

Figure n°3 shows the histogram of the output signal in the dark with the 210fF capacitance for a 30ms integration time and a reverse bias of 0,5V. The output signal in the dark turned out to be independent of the AlGaIn pixel and simply given by the read out current in the silicon readout circuit. The full width of half maximum actually describes the ROIC uniformity which is about 4%. Hence, most of the pixels (good pixels) present an output signal in the dark which does not depend on AlGaIn. In a few pixels (leaky pixels), the output level is found to be due to a leakage current in the AlGaIn diode. Then, the output level was monitored as a function of time. In good pixels, the standard deviation of the signal after analogic-numeric conversion is about 40e- rms for an integration time from 220 $\mu$ s to 3ms, and with the large gain setting. From the specifications the readout noise of the ISC 9809 ROIC is in the range of 40-70e-rms. Hence, the temporal noise is due to the ROIC. In addition, it does not depend on the integration time, showing that it is mainly due to the commutation of transistors in the ROIC. In leaky pixels, the temporal noise was larger, up to about 1200e- rms. This maximum noise corresponds to a dark current (or equivalently a R<sub>0</sub>A) that is about 150 times larger than the usual value mentioned earlier.

The dynamical behavior of the array was also checked by inspecting images of objects that were rapidly moving in the field of the camera. We did not see any evidence of hysteresis. In the spatial domain, we did not observe any blooming effect, showing that the optical cross is not a serious problem in AlGaIn arrays: this is actually not a surprise given the large absorption coefficient in AlGaIn and the relatively low optical index contrast between the AlGaIn layer in the sapphire substrate (2.3 and 1.8 respectively).

## 2. UV IMAGING FROM 360nm TO 260nm

Since the development of Wood' glass, ultraviolet (UV) imaging has known a constant but always confidential use. Different kinds of camera more or less adapted to UV wavelengths have been developed. When thinned, CCD has the capabilities to present large quantum efficiency in UV. Such devices have been developed for space applications and are now largely used in spectroscopy or microscopy. Photon counting based on electron multiplication in registers can also be achieved with EMCCD.

Nevertheless, UV imaging is not yet fully developed due to requirements of UV filters. Even with a long experience, such filters are not so

friendly to use. Consequently, there are reasons to develop UV solar blind detector like hybrid CMOS focal plane arrays (FPA). The hybrid-CMOS architecture is a competitor to CCD that can also achieve large quantum efficiency, low electrical noise and advanced functionalities<sup>1</sup> in image processing. AlGaN hybrid CMOS is an extension of this last technology we have developed for several years. Some new advantages have appeared since we currently employ AlGaN FPA. Indeed, imaging with such a narrow bandwidth is less prompt to chromatic aberration due to index dispersion in optics. For example the huge dispersion of index taking place in the ultraviolet range, even for UV compatible materials, requires a narrow band pass to prevent chromatic aberration or expensive dedicated optics. Hetero-structures based on different aluminum contents in alloys provide such band pass filtering of 10 to 20nm.

AlGaN based focal plan array are now integrated in standard supply chain. Our AlGaN based focal plane array is integrated in a packaging from 3-5 lab of 27.5mm x 20mm x 8.7mm (Figure). Single stage TE cooler (8.6V-5.7W) is integrated. The packaging is hermetically sealed by a sapphire window transmitting the UV radiation. In future development the window can be achieved from colored glasses (UG-5, UG-11, Hoya 330) in order to avoid UV radiation onto readout circuit and complete the rejection of visible. Even if filtering is required for solar blind imaging, specifications for designing filters are strongly relaxed below 300nm. Imaging capability and sharp cut-off will be achieved by the bandwidth defined by the AlGaN active and window layers. This narrow bandwidth is a key parameter to solve effects of index dispersion in optics.

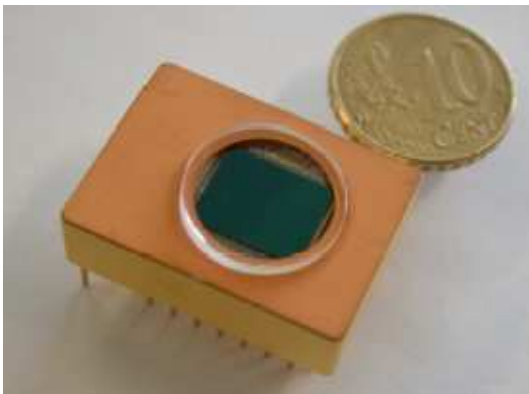


Fig. 4: Packaging dedicated to 320x256 FPA

Narrow bandwidth imaging can now follow a new development. Such cameras are sufficiently sensitive and UV selective to achieve imaging with a high visible background. This is attractive for several applications like imaging of biochips in UV-B, dermatology, dentistry and flame monitoring in the UV-A range.

**2.1. Outdoor imaging in the UV-A range**

Images have been recorded with various arrays. Outdoor imaging can be obtained without lighting in the UV-A range (400nm to 310nm) with an active layer made of GaN.



Fig. 5 : UV images of an outdoor scene at 360nm

**2.2. Imaging of flame at 310nm**

At larger wavelengths (310 nm), the camera was used to observe the flame of Bunsen burner. Figure 5 show the visible image and the UV image of the Bunsen burner





Fig. 6: UV of flamme at 310nm

## 2.2. Imaging of flame at 280nm

Solar blind images are limited to some special configuration. We have for instance checked the solar blindness in the image shown in Fig. 7. The camera is imaging the light emitted by a deuterium lamp at 1 m with the sun present in the back scene. As can be seen in Fig.7, the sun is not visible and the deuterium lamp is imaged. Note however that the image of the sun was not focused on the array: in this later case, the flux was large enough to saturate the camera. However, using of a basic black glass (Schott UG11) we could recover the image of the lamp without being bloomed by the sun.



Fig. 7: Image of a deuterium lamp (bright spot) at 290nm with the sun (invisible) in background.

## 2.4. Biological applications

Detection of biological macromolecules on a biochip dedicated to UV specific absorption has been developed<sup>5</sup>. It based on an ultraviolet biosensing technique based on specific molecular absorption detected with a previously developed spectrally selective AlGa<sub>0.65</sub>N based detector. Light absorption signal of DNA and proteins, respectively at 260 nm and 280 nm, is used to image biochips. To allow detection of protein or DNA monolayers at the surface of a biochip, we develop contrast-enhancing multilayer substrates. This label-free optical method may be helpful in controlling biochip coatings, and subsequent biological coupling at the surface of a biochip.

The capacity to detect ng/cm<sup>2</sup> of proteins has been demonstrated. Future design of biochips aims to achieve the detection in the range of pg/cm<sup>2</sup>

comparable to more complicated label-free detection setups<sup>6</sup>.

## 3. ROUTE TOWARD DEEP U.V.

The principal differences occurring when passing from UV A / UV B to deep UV imaging, is that lighting through the substrate is impossible. Indeed, all material are absorbing deep UV photons in few nanometers. We will first investigate topside illumination and then demonstrate how deep UV imaging can be extended in backside illumination configuration compatible with standard hybridization schemes.

### 3.1. Process for topside illuminated detector

Measurements in front side illumination have already been carried out on Metal-Semiconductor-Metal (MSM) grown on layers with high aluminium contents (>75%). Metallization for Schottky contacts consists in 5nm of platinum plus 5nm of gold. Simulations with IMD software predict a transmission from 20 to 30% for the range of wavelengths studied (from 60nm to 30nm). These contacts are semi-transparent in order to take advantage of absorption and electrical responsivity under the metal layer. Contact pads are deposited just behind on a silicon dioxide layer in order to avoid electrical leakage and contribution of contacts pads to photocurrent. This oxide has to be removed on inter-digitised fingers not to absorb deep UV photons. Reactive Ion Etching etches silica in order to release AlGa<sub>0.65</sub>N surface after contact pad on SiO<sub>2</sub> definition.

The results have been published previously<sup>3</sup>. Deep UV reponsivity had been generated with an attosecond generation in gas plasma (Argon, Krypton, Xenon...). Some details about the experimental setup are described this reference. Spectra are made of even harmonics of the primary laser at 800nm. The intensity depends of the gas injected for coherent generation. We used essentially krypton to intense harmonics down to 38nm. This experiment revealed an important contribution from internal photoemission in metal.

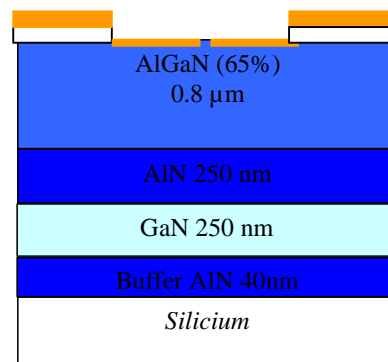


Fig. 8: Layers and process for topside illumination.

### 3.2. Backside illumination for deep U.V.

When considering mono-element pixel detection, photo-emission from metal is not a problem. Electrons extracted from metal contribute to the quantum efficiency of detectors before being collected by materials somewhere in the close environment. On the contrary, in the case of an array of close pixels, the collection of electrons by neighbor pixels will disturb the Modulation Transfert Function of the FPA. An easy way to solve both MTF troubles and being compatible with hybridisation to ROIC process is to remove substrate and window layer. Techniques like thinning, removal of the substrate, sacrificial layer, smart-cut, throw the wafer connection are also possible. We show here after the possibility to process GaN on silicon layers with etching processes developed for micro-machining (Bosch process). It can provide a robust AlGaN membrane or a honeycomb structure before specific window layers etching. Membranes of one micrometer of thickness and several millimetres of length have been achieved. It presented curvature due to stress but backside etching would be possible when samples are glued to hoste substrate.

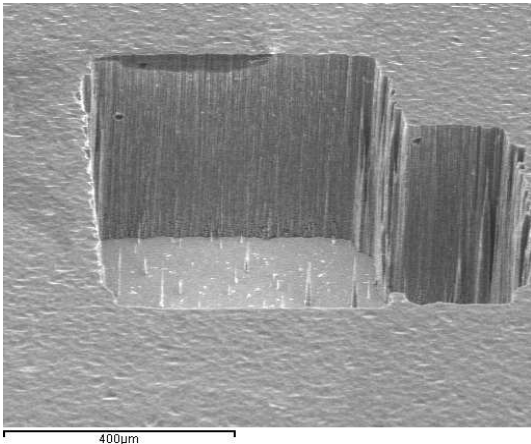


Fig 9: GaN membrane release after Bosch process showing the rigidity of a 250nm thick membrane

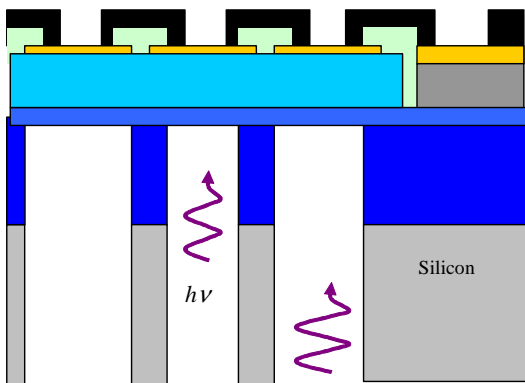


Fig 10: Etching of silicon substrate in order to achieve backside illumination.

### 3.3. Strategy to go adapt the current near UV technology to deep UV

MSM structures (without gradual alloys and doping) have been obtained on silicon with the same equivalent aluminium content present on sapphire. It shown the same results as those published for deep-UV in reference in front side illumination<sup>3</sup>. Cracks can occurs when the temperature of layers decreases from growth temperature to room temperature. These cracks are avoided by a GaN / AlN multilayer structure at the bottom of the epitaxy<sup>7</sup>.

AlGaN (44%) 0.6 $\mu$ m
AlGaN 0.2 $\mu$ m 63%=>44%
AlGaN (63%) 1 $\mu$ m / 2.10 <sup>19</sup> cm <sup>-3</sup>
AlN 250 nm
GaN 250 nm
Buffer AlN 40nm
Silicium

Fig. 11: Schottky photodiodes for deep UV

The 2D array will be hybridized to the same readout circuit used for InGaAs and near UV. It is a 320 x 256 pixels with a pitch of 30 $\mu$ m. Neither specific design nor post-processing of the readout circuit (shielding and screening against visible light and high energy) will be implemented. Even though, solar mission specifications requires development of 2k x 2k pixels arrays with a pitch of 10 $\mu$ m, the objective is here only to test the capability to collect carriers created on the backside of the AlGaN membrane.

Steps to eliminate the substrate and basal layers of AlGaN epilayers are described as followed.

### 3.4. Hybridisation to readout and polishing of silicon substrate

The silicon part of an hybrid can be polished down to 10 to 20 $\mu$ m of thickness as shown in figure 12. In this case it is the readout circuit that is polished down to 20  $\mu$ m and the AlGaN on sapphire substrate is kept at 300 $\mu$ m. The reader can appreciate the expected difficulties due to the stress accumulated in the different layers. Success of the membrane release lie in the capability of indium bump sealed in the under filling polymer to resist during polishing, wet and dry etching of the membrane. Such membranes are often employed for Infrared technologies in order to avoid the effects of thermal cycling and especially stress between readout circuit and 2D array.



Fig. 12: SEM image of a polished readout circuit hybridized to an AlGaIn on sapphire 2D array.

EDP (Ethylène Diamine Pyrocatechol) or KOH will remove the remaining silicon layer. The resulting etching is anisotropic and is more adapted to the (100) face of silicon than the (111) face involved as substrate for GaN growth. In our case we will prefer isotropic solution based on HF, HNO<sub>3</sub> and H<sub>2</sub>O.

### 3.5. Etching of basal AlGaIn layer

In the case of layers depicted in figure n°11, the basal layers must be removed. The crystallographic phase of (Al,Ga)N layers are currently Wurtzite. Whereas the gallium side oriented from the substrate to the top is extremely stable, the nitrogen side of the wurtzite layers can be etched more easily.

Solution based on KOH, H<sub>3</sub>PO<sub>4</sub>, and NaOH are common solution for wet etching<sup>8</sup>. Some developer (AZ400 in which the active component is KOH) employed in lithography are also known to etch the wurtzite layers<sup>9</sup>. Another solution is to develop a band-gap selective photo-electrochemical etching<sup>10</sup>. It is a potential way to stop etching at a level optimized for collection of carriers. Moreover this stop etching must minimize surface recombination taking place in the backside surface of membrane.

Another solution is a dry etching based on ICP (Inductively Coupled Plasma). These plasmas are used to define the mesa in the 2D array of photodiodes. Like the other dry etching, they are more homogenous than wet etching. The key parameter is to control the temperature lower than the 80°C limit due to the indium bump. Short steps of etching could be a solution to avoid thermal effects.

## 4. CONCLUSION

The supply chain of AlGaIn on sapphire based imaging is now achieved. It can compete with technologies based on photocathodes, MCP intensifiers, back-thinned CCD or hybrid CMOS FPA for low flux measurements. AlGaIn based

cameras allow UV imaging without filters or with simplified ones. UV camera with detection band from 360nm to 260nm can now be sampled.

Replacing sapphire substrate by silicon is an interesting way to extend the technology in a standard semiconductor industry. Moreover, this substrate is cheaper, compatible with large wafer foundry and can easily be removed by polishing and wet etching. To achieve substrate removing and membrane releasing is a convenient way to extend sensitivity to deep-UV. It is the objective of a new R&T project financed by CNES.

If consistent quantum efficiency is achieved, the next steps will concern the realization of specific readout circuit. Such a readout circuit specific to ultraviolet optical budget will concern shielding and a spatial definition compatible with solar imaging: 2k x 2k pixels with a 10µm pitch.

## 4. ACKNOWLEDGMENT

The author acknowledge a financial support from the ANR-05-Blan0393 project SYNCHROGAN and the CCTP n°R-S08SU-0004-029 from CNES

## 5. REFERENCES

- <sup>1</sup> J-L Reverchon, G. Mazzeo, A. Dussaigne and J.Y. Duboz Proc. of SPIE Vol. (2005)
- <sup>2</sup> R. McClintock, K. Mayes, A. Yasan, D. Shiell, P. Kung, and M. Razeghi, Appl. Phys. Lett. **86**, 011117-1 (2005).
- <sup>3</sup> J-L. Reverchon, J-A. Robot, J-P. Truffer, J-P. Caumes, I. Mourad, J. Brault, J-Y. Duboz, Proc. SPIE n°6744-9 (2007)
- <sup>4</sup> J-Y Duboz, J. Brault, J-P. Truffer, J-A. Robot, K. Robin, J-L. Reverchon, Proc. IWN (2008)
- <sup>5</sup> K. Robin, J-L Reverchon, L. Mughlerli, Michel Fromant, P. Plateau, H. Benisty, Biosensors and Bioelectronics Accepted for publication (2008)
- <sup>6</sup> Smith, E.A., Corn, R.M., 2003. Appl. Spectrosc. **57** (11), 320–332.
- <sup>7</sup> Y. Cordier et al. Phys. stat. Sol. (c) 0, No. 1, 61–64 (2002)
- <sup>8</sup> Stocker et al. Appl. Phys. Lett., Vol. 73, No. 18, November 1998
- <sup>9</sup> J.R Mileham et al., Appl. Phys. Lett., Vol. 67, No. 8, August 1995
- <sup>10</sup> Haberer et al., Appl. Phys. Lett., Vol. 85, No. 5, August 2004